Journal of Mathematical Biology (2021) 83:15
https://doi.org/10.1007/s00285-021-01640-z

Mathematical Biology

A model of algal growth depending on nutrients and inorganic carbon in a poorly mixed water column

Jimin Zhang[1] · Junping Shi[2] · Xiaoyuan Chang[3]

Received: 16 July 2020 / Revised: 24 June 2021 / Accepted: 27 June 2021

Abstract
A reaction-diffusion-advection model is proposed to describe the growth of algae depending on both nutrients and inorganic carbon in a poorly mixed water column. Nutrients from the water bottom and inorganic carbon from the water surface form an asymmetric resource supply mechanism for the algal growth. The existence and stability of semi-trivial steady state and positive steady state of the model are proved, and a threshold condition for the regime shift from extinction to survival of algae is established. The influence of environmental parameters on the vertical distribution of algae is investigated in the water column. It is shown that the vertical distribution of algae can exhibit many different profiles under the combined limitation of nutrients and inorganic carbon.

Keywords Reaction-diffusion-advection model · Effect of nutrients and inorganic carbon · Vertical distribution of algae · Environmental parameters

Mathematics Subject Classification 35J25 · 92D25 · 35A01

Partially supported by NSFC-11971088, NSFC-11901140, NSFHLJ-LH2019A022, and NSF-DMS-1853598.

✉ Junping Shi
jxshix@wm.edu

[1] School of Mathematical Sciences, Heilongjiang University, Harbin, Heilongjiang 150080, People's Republic of China

[2] Department of Mathematics, William & Mary, Williamsburg, VA 23187-8795, USA

[3] School of Science, Harbin University of Science and Technology, Harbin, Heilongjiang 150080, People's Republic of China

Published online: 08 July 2021

1 Introduction

Algae are the basis of the earth's food web and preserve the balance of the global aquatic ecosystem. They are adaptable and widely distributed in rivers, lakes and oceans. By performing photosynthesis, algae consume inorganic carbon to produce organic matter and release oxygen by using light energy. In this process, inorganic carbon and light are involved in the energy flow and material cycle of the aquatic ecosystem. Nutrient elements, such as phosphorus or nitrogen, are key factors for algal growth and important indicators of water eutrophication. Therefore the growth of algae is supported and restricted by three essential resources: light, nutrients (e.g. nitrogen or phosphorus) and inorganic carbon (including dissolved CO_2, carbonic acid and bicarbonate). Understanding algal growth in an aquatic environment is of fundamental importance to ecosystem studies.

Mathematical models have been constructed to study the growth mechanism of algae and its dependence on algae and nutrients, or light, or both of them. Three different situations have been studied and discussed. First, algae compete only for nutrients in oligotrophic aquatic ecosystems with ample supply of light (Hsu et al. 2013; Nie et al. 2015; Shi et al. 2019; Wang et al. 2015; Zhang et al. 2018); second, algae compete only for light in eutrophic aquatic ecosystems (Du and Hsu 2010; Du et al. 2015; Hsu and Lou 2010; Jiang et al. 2019; Mei and Zhang 2012; Peng and Zhao 2016); third, algae compete for both light and nutrients simultaneously in some aquatic ecosystems (Chen et al. 2015; Du and Hsu 2008a, b; Huisman et al. 2006; Jäger et al. 2010; Klausmeier and Litchman 2001; Ryabov et al. 2010; Vasconcelos et al. 2016; Yoshiyama et al. 2009; Yoshiyama and Nakajima 2002; Zagaris and Doelman 2011; Zhang et al. 2021).

The connection between algae and inorganic carbon is more complicated with a variety of biological mechanisms. Carbon dioxide enters the water by exchange at the water surface, and reacts with water molecules to form carbonic acid and bicarbonate. Algae could take up dissolve CO_2, carbonic acid and bicarbonate by photosynthesis. An ODE model was constructed in Van de Waal et al. (2011) to describe supply for dissolved inorganic carbon in dense algal blooms in a completely well-mixed water column. In Nie et al. (2016) and Hsu et al. (2017), the authors established PDE models to deal with the interaction between algae and inorganic carbon in a poorly mixed habitat.

The main purpose of this paper is to establish a mathematical model to describe the interaction of algae, nutrients and inorganic carbon in a poorly mixed water column with ample supply of light. The growth of algae only depends on nutrients from the bottom and inorganic carbon from the surface (see Fig. 1). The increase of the algal biomass on the water surface inhibits the algal growth on the deep layer since limited inorganic carbon from the surface decreases its supply to the deep layer. On the other hand, an increase of the algal biomass on the water bottom also suppresses the algal growth in the surface layer since limited nutrients from the water bottom decreases its supply to the surface layer. This forms an asymmetric supply for the algae to gain the two resources. It is important and of interest to explore the effect of this asymmetric resource supply for nutrients and inorganic carbon on the algal growth and vertical distribution.

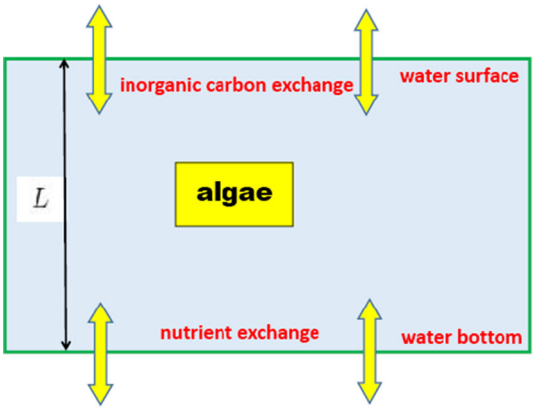

Fig. 1 Interactions of algae, nutrients and inorganic carbon in a water column

The vertical distribution of algae is highly heterogeneous and exhibits the most prominent vertical aggregation phenomena. For example, algae usually float on the water surface during the daytime and sink to the water bottom at night. The spatial heterogeneity of algae is generally related to the uneven distribution of essential resources. Previous studies have shown that algae have complex vertical distribution that is influenced by the supply of light and nutrients in poorly mixed water columns (Du and Hsu 2008a, b; Klausmeier and Litchman 2001; Ryabov et al. 2010; Yoshiyama et al. 2009; Yoshiyama and Nakajima 2002). Here we consider a controlled water column in the experiment or an idealized water column, where the whole water column receives enough light. Therefore, in the present paper, assuming that light is sufficient, we will reveal that algae also exhibit vertical spatial heterogeneity and vertical aggregation phenomena under asymmetric resource supply mechanism of nutrients and inorganic carbon, which has not been considered in previous studies.

The rest of the paper is organized as follows. In Section 2, we derive a reaction-diffusion-advection PDE model to describe the growth of algae depending on both nutrients and inorganic carbon in a poorly mixed water column. We then investigate the basic dynamics of this model including the existence and stability of steady states in Section 3. In Section 4, we consider the influence of environmental parameters on the vertical distribution of algae, and explain what mechanisms drive these vertical distributions. Finally, we summarize our findings and state some questions for future study in Section 5. Throughout the paper, numerical simulations under reasonable parameter values from literature are presented to illustrate or complement our mathematical findings.

2 Model construction

In this section, we propose a mathematical model to describe the interactions of algae, nutrients and inorganic carbon in a poorly mixed water column (see Fig. 1). Nutrients from the bottom and inorganic carbon from the water surface constitute an asymmetric resource supply in terms of different spatial niche. This paper mainly considers the

Table 1 Variables and parameters of model (2.4) with biological meanings

Symbol	Meaning	Symbol	Meaning
t	Time	z	Depth
A	Biomass density of algae	N	Concentration of dissolved nutrients
C	Concentration of dissolved inorganic carbon	D_a	Vertical turbulent diffusivity of algae
D_n	Vertical turbulent diffusivity of dissolved nutrients	D_c	Vertical turbulent diffusivity of dissolved inorganic carbon
s	Sinking or buoyant velocity of algae	r	Maximum specific production rate of algae
m	Loss rate of algae	l	Respiration rate of algae
γ_n	Half saturation constant for nutrient-limited production of algae	γ_c	Half saturation constant for inorganic carbon-limited production of algae
c_n	Phosphorus to carbon quota of algae	p_n	Proportion of nutrient in algal losses that is recycled
p_c	The proportion of carbon dioxide released by algae respiration in the water column	α	Nutrient exchange rate at the bottom of the water column
β	CO_2 gas exchange rate between air and water at the surface of the water column	N^0	Concentration of dissolved nutrients at the bottom of the water column
C^0	Concentration of dissolved inorganic carbon at the surface of the water column	L	Depth of the water column

growth/extinction of algae and their vertical distribution under the framework of asymmetric supply. In order to obtain the main research objectives of the present paper, we assume that the poorly mixed water column is an idealized or a controlled one in the experiment. For example, the water column is in a glass aquarium holding water, and it receives abundant and even light from the side. Therefore, in the following modeling process, the factor of light is not emphasized (assuming that the light is sufficient and constant for the whole water column), and only the limitation of nutrients and inorganic carbon on algal growth is considered.

Let z denote the depth coordinate of the water column. We assume that $z = 0$ is the surface of the water column, and $z = L$ is the bottom of the water column. Three partial differential equations are established below to describe the dynamics of biomass density of algae A, concentration of dissolved nutrients N (e.g. nitrogen or phosphorus), and concentration of dissolved inorganic carbon C (including dissolved CO_2, carbonic acid and bicarbonate). All the variables and parameters of the model and their biological significance are listed in Table 1.

Let $A(z, t)$ denote the biomass density of algae at depth $z \in [0, L]$ and time t. The growth rate of algae has two limiting factors: concentration of dissolved nutrients $N(z, t)$ and concentration of dissolved inorganic carbon $C(z, t)$. Nutrients mainly contains trace elements such as phosphorus or nitrogen, and inorganic carbon is necessary for algae photosynthesis, so both of them are irreplaceable resources for algal

growth. Here we assume the algae growth rate takes a form of multiplication of two Monod type functions depending on the two resources:

$$f(N)g(C) = \frac{N}{\gamma_n + N}\frac{C}{\gamma_c + C},$$

where γ_n and γ_c are half saturation constants. This form of multiplication of two resource functions has been used in previous studies (see Heggerud et al. 2020; Wang et al. 2007; Zagaris and Doelman 2011). The other commonly used algebraic form for modeling two irreplaceable resources is the minimum value of two resource functions $\min\{f(N), g(C)\}$ based on Liebig's law of the minimum (see Du and Hsu 2008a, b; Hsu et al. 2016; Klausmeier and Litchman 2001; Klausmeier et al. 2004). The two functions are qualitatively similar in the sense that $f \cdot g \leq \min\{f, g\} \leq \sqrt{f \cdot g}$ as $0 \leq f, g \leq 1$ while the value of the multiplicative function is smaller than the one of the minimum function. From the biological point of view, the multiplication form or the minimum form means that nutrients and inorganic carbon are two essential resources for algal growth, which cannot be substituted by each other Grover (1997). We use the multiplicative form here as it is a differentiable function which is more convenient for mathematical analysis.

It is assumed that algae biomass density is lost at a density-independent rate m, caused by death and grazing, and respiration rate l, caused by the respiration of algae (Hsu et al. 2017; Nie et al. 2016). On the other hand, algae move up or down by turbulence with a depth independent diffusion coefficient D_a. In addition, algae sink or buoyant with a velocity s. In most cases, algae sink due to the gravity ($s > 0$); in order to obtain better growth opportunities, algae suspend in water by increasing their own buoyancy ($s = 0$); and some algae can produce pseudovacuoles, store light density lipids, and make their buoyancy greater than their body weight, resulting in buoyancy ($s < 0$) (Grover 2017; Klausmeier and Litchman 2001). Realistic advective term would depend on the space and time, here we assume the sink/buoyant velocity s to be a constant as the mean value over space and time for simplicity (Huisman et al. 2006; Jäger et al. 2010; Ryabov et al. 2010). No-flux boundary conditions are imposed for algae at both the water surface and the bottom of the water column. Combining these assumptions gives the following reaction-diffusion-advection equation with no-flux boundary conditions:

$$\begin{aligned}\frac{\partial A(z,t)}{\partial t} &= \text{turbulent diffusion} - \text{sinking(or buoyant)} + \text{growth} - \text{loss},\\ &= D_a\frac{\partial^2 A}{\partial z^2} - s\frac{\partial A}{\partial z} + rf(N)g(C)A - (m+l)A, \quad 0 < z < L,\\ &\quad D_a A_z(0,t) - sA(0,t) = 0,\ D_a A_z(L,t) - sA(L,t) = 0. \end{aligned} \tag{2.1}$$

The function $N(z,t)$ describes the concentration of dissolved nutrients in the water column at depth $z \in [0, L]$ and time t. We assume a zero-flux boundary condition for nutrients at the water surface, while nutrients are supplied from the bottom of the water column with a fixed concentration N^0 and nutrient exchange rate α. The nutrient transport is also governed by passive movement due to turbulence with a

diffusion coefficient D_n. Nutrients are consumed by algae with a consumption rate $c_n r f(N) g(C) A$, and they are generated as a result of recycling from loss of algal biomass with proportion $p_n \in [0, 1]$. The dynamics of $N(z, t)$ is given by

$$\begin{aligned}\frac{\partial N(z,t)}{\partial t} &= \text{turbulent diffusion} + \text{recycling} - \text{consumption}\\ &= D_n \frac{\partial^2 N}{\partial z^2} + p_n c_n m A - c_n r f(N) g(C) A,\ 0 < z < L,\\ N_z(0,t) = 0,\ D_n N_z(L,t) &= \alpha(N^0 - N(L,t)) \text{ (nutrients exchange).}\end{aligned} \tag{2.2}$$

Let $C(z, t)$ be the concentration of dissolved inorganic carbon in the water column at depth $z \in [0, L]$ and time t. Inorganic carbon in the water column mainly comes from the atmosphere, and a very small part comes from the sediment. In order to study the asymmetry of resource supply in the present paper, we assume that inorganic carbon is only supplied from the atmosphere at the surface of the water column with a fixed concentration C^0 and CO_2 gas exchange rate β. The transport of inorganic carbon in the water column is also controlled by turbulence with a diffusion coefficient D_c. The change of dissolved inorganic carbon depends on consumption by algae with a consumption rate $r f(N) g(C) A$, recycling from respiration of algae with proportion $p_c \in [0, 1]$. The dynamics of $C(z, t)$ is described as

$$\begin{aligned}\frac{\partial C(z,t)}{\partial t} &= \text{turbulent diffusion} + \text{recycling} - \text{consumption}\\ &= D_c \frac{\partial^2 C}{\partial z^2} + p_c l A - r f(N) g(C) A,\ 0 < z < L,\\ D_c C_z(0,t) = \beta(C(0,t) - C^0) &\ (CO_2 \text{ exchange}),\ C_z(L,t) = 0.\end{aligned} \tag{2.3}$$

Combining all equations (2.1)-(2.3), we have the following full system of algae-nutrient-inorganic carbon model:

$$\begin{cases}\dfrac{\partial A}{\partial t} = D_a \dfrac{\partial^2 A}{\partial z^2} - s \dfrac{\partial A}{\partial z} + r f(N) g(C) A - (m + l) A, & 0 < z < L,\ t > 0,\\ \dfrac{\partial N}{\partial t} = D_n \dfrac{\partial^2 N}{\partial z^2} + p_n c_n m A - c_n r f(N) g(C) A, & 0 < z < L,\ t > 0,\\ \dfrac{\partial C}{\partial t} = D_c \dfrac{\partial^2 C}{\partial z^2} + p_c l A - r f(N) g(C) A, & 0 < z < L,\ t > 0,\\ D_a A_z(0,t) - s A(0,t) = 0,\ D_a A_z(L,t) - s A(L,t) = 0, & t > 0,\\ N_z(0,t) = 0,\ D_n N_z(L,t) = \alpha(N^0 - N(L,t)), & t > 0,\\ D_c C_z(0,t) = \beta(C(0,t) - C^0),\ C_z(L,t) = 0, & t > 0.\end{cases} \tag{2.4}$$

In the model (2.4), one of the two resources (nutrients and inorganic carbon) diffuses in from one side, and the other one diffuses from the other side (also with advective transport), which resembles a counter-diffusion system. It characterizes the growth of algae under the asymmetric supply mechanism of nutrients and inorganic carbon.

Due to the biological meaning of variables in (2.4), we will deal with the solutions of (2.4) with nonnegative initial values, i.e.

$$A(z,0) = A_0(z) \geq\not\equiv 0,\ N(z,0) = N_0(z) \geq\not\equiv 0,\ C(z,0) = C_0(z) \geq\not\equiv 0.$$

The symbol $\geq\not\equiv 0$ means that a function is non-negative and at least one point is strictly positive. We also assume that $s \in \mathbb{R}$, p_n, $p_c \in [0,1]$ and all remaining parameters are positive constants unless explicitly stated otherwise. In order to describe the growth and extinction of algae under asymmetric resource supply, we will analyze the steady state solutions of model (2.4) in the next section.

3 Existence and stability of steady states

In this section, we consider the existence and stability of steady state solutions of (2.4).

A nutrient-inorganic carbon-only trivial steady state $E_1 : (0, N_1(z), C_1(z))$ satisfies

$$\begin{cases} N''(z) = 0,\ N'(0) = 0,\ D_n N'(L) = \alpha(N^0 - N(L)), & 0 < z < L, \\ C''(z) = 0,\ D_c C'(0) = \beta(C(0) - C^0),\ C'(L) = 0, & 0 < z < L. \end{cases} \tag{3.1}$$

We have the following results regarding the existence, uniqueness and stability of E_1.

Theorem 3.1 *(i) The system (2.4) has a unique nutrient-inorganic carbon-only steady state solution $E_1 \equiv (0, N^0, C^0)$;*

(ii) If

$$m + l > rf(N^0)g(C^0), \tag{3.2}$$

then E_1 is locally asymptotically stable with respect to (2.4), and if

$$m + l < rf(N^0)g(C^0), \tag{3.3}$$

then E_1 is unstable;

(iii) If

$$m + l > r, \tag{3.4}$$

or $p_n = p_c = 0$ and (3.2) hold, then E_1 is globally asymptotically stable with respect to (2.4) for any nonnegative initial value.

Proof It follows from (3.1) that (i) holds. The stability of E_1 is determined by the eigenvalue problem

$$\lambda\varphi(z) = D_a\varphi''(z) - s\varphi'(z) + \left[rf(N^0)g(C^0) - (m+l)\right]\varphi(z),\ 0 < z < L, \tag{3.5a}$$

$$\lambda\psi(z) = D_n\psi''(z) + c_n(p_n m - rf(N^0)g(C^0))\varphi(z),\ 0 < z < L, \tag{3.5b}$$

$$\lambda\phi(z) = D_c\phi''(z) + (p_c l - rf(N^0)g(C^0))\varphi(z),\ 0 < z < L, \tag{3.5c}$$

$$D_a\varphi'(0) - s\varphi(0) = D_a\varphi'(L) - s\varphi(L) = 0, \tag{3.5d}$$

$$\psi'(0) = 0,\ D_n\psi'(L) + \alpha\psi(L) = 0, \tag{3.5e}$$

$$-D_c\phi'(0) + \beta\phi(0) = 0,\ \phi'(L) = 0. \tag{3.5f}$$

Let λ be any eigenvalue of (3.5), and let (φ, ψ, ϕ) be the corresponding eigenfunction. Note that the linearized system (3.5) is partially decoupled. We consider the following two cases: $\varphi \neq 0$ and $\varphi \equiv 0$.

Case 1: $\varphi \neq 0$. In this case, the stability of E_1 is determined by (3.5a) and its boundary condition (3.5d). Let $\varphi = e^{(s/D_a)z}\eta$. Then (3.5a)-(3.5d) translates into

$$\begin{cases} \lambda\eta(z) = D_a\eta''(z) + s\eta'(z) + \left[rf(N^0)g(C^0) - (m+l)\right]\eta(z), & 0 < z < L, \\ \eta'(0) = \eta'(L) = 0. \end{cases} \tag{3.6}$$

It is not difficult to show that the dominant eigenvalue of (3.6) is $rf(N^0)g(C^0) - (m + l)$ and the corresponding eigenfunction is $\eta(z) \equiv 1$. This implies that $\lambda = rf(N^0)g(C^0) - (m+l)$ is also an eigenvalue of (3.5), the corresponding eigenfunction is $\varphi(z) = e^{(s/D_a)z}$, and (ψ, ϕ) can be solved from (3.5).

Case 2: $\varphi \equiv 0$. In this case, (3.5b) and (3.5c) with their boundary conditions (3.5e) and (3.5f) reduce to

$$\lambda\psi(z) = D_n\psi''(z),\ 0 < z < L,\ \psi'(0) = 0,\ D_n\psi'(L) + \alpha\psi(L) = 0, \tag{3.7}$$

and

$$\lambda\phi(z) = D_c\phi''(z),\ 0 < z < L,\ -D_c\phi'(0) + \beta\phi(0) = 0,\ \phi'(L) = 0. \tag{3.8}$$

The eigenvalues of (3.7) must be negative. In fact, if $\lambda > 0$ in (3.7), then we have $\psi(z) = \cosh(\sigma z)$ for $\sigma = \sqrt{\lambda/D_n}$ since $\psi'(0) = 0$. But from $D_n\psi'(L) + \alpha\psi(L)$=0, we obtain $D_n \sinh(\sigma L) = -\alpha\cosh(\sigma L)$, which is a contradiction. It is also easy to see $\lambda = 0$ cannot be an eigenvalue of (3.7). If $\lambda < 0$, then from $\psi'(0) = 0$ we have $\psi(z) = \cos(\sigma z)$ for $\sigma = \sqrt{-\lambda/D_n}$. It follows from $D_n\psi'(L) + \alpha\psi(L) = 0$ that $\tan\sigma L = \alpha/(\sigma D_n)$. Then the dominant eigenvalue of (3.7) is $\lambda = -D_n\sigma_1^2$, where σ_1 is the smallest positive root of $\tan\sigma L = \alpha/(\sigma D_n)$. Similarly, the eigenvalues of (3.8) are also negative.

Summarizing above discussions, we conclude that all eigenvalues of (3.5) are negative if (3.2) holds, and then E_1 is locally asymptotically stable. On the other hand, if (3.3) holds, then E_1 is unstable. Therefore, (ii) holds.

We now prove the global stability in (iii). First we assume that (3.4) holds. From the first equation of (2.4) and (3.4), we have

$$\frac{\partial A}{\partial t} \leq D_a\frac{\partial^2 A}{\partial z^2} - s\frac{\partial A}{\partial z} + (r - (m+l))\,A,\ 0 < z < L,\ t > 0, \tag{3.9}$$

which implies that $A(z,t)$ converges to 0 uniformly for $z \in [0,L]$ as $t \to \infty$ by the comparison theorem of parabolic equations. It follows from the theory of asymptotic autonomous systems (see Theorem 1.8 in Mischaikow et al. (1995) or Theorem 4.1 of Thieme (1992)) that the dynamics of (2.4) reduces to the one of limiting system

$$\begin{cases} \dfrac{\partial N}{\partial t} = D_n \dfrac{\partial^2 N}{\partial z^2}, & 0 < z < L,\ t > 0, \\ \dfrac{\partial C}{\partial t} = D_c \dfrac{\partial^2 C}{\partial z^2}, & 0 < z < L,\ t > 0, \\ N_z(0,t) = 0,\ D_n N_z(L,t) = \alpha(N^0 - N(L,t)), & t > 0, \\ D_c C_z(0,t) = \beta(C(0,t) - C^0),\ C_z(L,t) = 0, & t > 0. \end{cases} \tag{3.10}$$

To obtain our conclusions, we define the following Lyapunov functional $V : C([0,L]) \times C([0,L]) \to \mathbb{R}$ by

$$V(N,C) = \frac{1}{2}\int_0^L (N(z) - N^0)^2 dz + \frac{1}{2}\int_0^L (C(z) - C^0)^2 dz.$$

Let $(N(z,t), C(z,t))$ be an arbitrary solution of (3.10) with nonnegative initial values. Then

$$\begin{aligned} \frac{dV(N(z,t),C(z,t))}{dt} &= \int_0^L (N(z,t) - N^0)\frac{\partial N}{\partial t} dz + \int_0^L (C(z,t) - C^0)\frac{\partial C}{\partial t} dz \\ &= D_n \int_0^L (N(z,t) - N^0)\frac{\partial N^2}{\partial z^2} dz \\ &\quad + D_c \int_0^L (C(z,t) - C^0)\frac{\partial C^2}{\partial z^2} dz \\ &= D_n \frac{\partial N}{\partial z}(N(z,t) - N^0)\Big|_0^L - D_n \int_0^L \left(\frac{\partial N}{\partial z}\right)^2 dz \\ &\quad + D_c \frac{\partial C}{\partial z}(C(z,t) - C^0)\Big|_0^L - D_c \int_0^L \left(\frac{\partial C}{\partial z}\right)^2 dz \\ &= -\alpha(N(z,t) - N^0)^2 - D_n \int_0^L \left(\frac{\partial N}{\partial z}\right)^2 dz \\ &\quad - \beta(C(z,t) - C^0)^2 - D_c \int_0^L \left(\frac{\partial C}{\partial z}\right)^2 dz \le 0. \end{aligned}$$

Note that $dV(\cdot)/dt = 0$ holds if and only if $N(z,t) \equiv N^0$ and $C(z,t) \equiv C^0$. From the LaSalle's Invariance Principle (Henry 1981, Theorem 4.3.4), we conclude that $(N(z,t), C(z,t))$ converges to (N^0, C^0) uniformly for $z \in [0,L]$ as $t \to \infty$. This means that E_1 is globally asymptotically stable with respect to (2.4) for any nonnegative initial value.

At last we prove the global stability of E_1 when $p_n = p_c = 0$ and (3.2) hold. From (2.4), we have

$$\begin{cases} \dfrac{\partial N}{\partial t} \le D_n \dfrac{\partial N^2}{\partial z^2}, & 0 < z < L,\ t > 0, \\ \dfrac{\partial C}{\partial t} \le D_c \dfrac{\partial^2 C}{\partial z^2}, & 0 < z < L,\ t > 0, \\ N_z(0,t) = 0,\ D_n N_z(L,t) = \alpha(N^0 - N(L,t)), & t > 0, \\ D_c C_z(0,t) = \beta(C(0,t) - C^0),\ C_z(L,t) = 0, & t > 0. \end{cases}$$

By using the comparison principle of parabolic equations, we get

$$\limsup_{t\to\infty} N(z,t) \le N^0,\ \ \limsup_{t\to\infty} C(z,t) \le C^0,\ 0 \le z \le L.$$

It follows from the first equation of (2.4) that for t large, we have

$$\frac{\partial A}{\partial t} \le D_a \frac{\partial^2 A}{\partial z^2} - s\frac{\partial A}{\partial z} + \left(rf(N^0+\varepsilon)g(C^0+\varepsilon) - (m+l)\right)A,\ 0 < z < L,$$

where $\varepsilon > 0$ is arbitrarily small. Then $A(z,t)$ converges to 0 uniformly for $z \in [0, L]$ as $t \to \infty$ if (3.2) holds. The rest of the proof is similar to the proof when (3.4) holds. □

The condition (3.2) shows that a large algal loss rate m or respiration rate l leads to the extinction of algae population, and such extinction is global for all initial conditions if $m + l$ is even larger. On the other hand, when m and l are both small, the extinction state E_1 is unstable and it is possible to have positive steady states (see Theorem 3.3). Another case of global stability of E_1 occurs when there is no recycling of nutrients and carbon dioxide in the system. It is an interesting question whether E_1 is also globally asymptotically stable for p_n, $p_c \neq 0$ if (3.2) holds, which is indicated by our numerical simulations.

Next we consider the existence of positive steady states of model (2.4). A positive steady state solution $E_2 : (A(z), N(z), C(z))$ of model (2.4) satisfies

$$\begin{cases} D_a A''(z) - sA'(z) + rf(N(z))g(C(z))A(z) - (m+l)\,A(z) = 0, & 0 < z < L, \\ D_n N''(z) + p_n c_n m A(z) - c_n rf(N(z))g(C(z))A(z) = 0, & 0 < z < L, \\ D_c C''(z) + p_c l A(z) - rf(N(z))g(C(z))A(z) = 0, & 0 < z < L, \\ D_a A'(0) - sA(0) = D_a A'(L) - sA(L) = 0, \\ N'(0) = 0,\ D_n N'(L) = \alpha(N^0 - N(L)), \\ D_c C'(0) = \beta(C(0) - C^0),\ C'(L) = 0 \end{cases} \tag{3.11}$$

and each of $A(z)$, $N(z)$ and $C(z)$ is positive. Assume that

$$m_* = rf(N^0)g(C^0) - l > 0. \tag{3.12}$$

We consider the bifurcation of the positive steady state E_2 from nutrients-inorganic carbon-only trivial steady state E_1 at $m = m_*$ by using bifurcation theory (see Crandall and Rabinowitz 1971, Theorem 1.7 and Shi and Wang 2009, Theorem 3.3 and Remark 3.4). Let

$$\begin{aligned} &\bar{\varphi}(z) = e^{(s/D_a)z},\ \bar{\psi}(z) = c_1 e^{(s/D_a)z} + c_2 z + c_3, \\ &\bar{\phi}(z) = \frac{D_a^2 m_*}{D_c s^2} e^{(s/D_a)z} + c_4 z + c_5,\ 0 < z < L, \end{aligned} \tag{3.13}$$

where

$$\begin{aligned} c_1 &= \frac{D_a^2(l + m_*(1 - p_n))}{D_n s^2},\ c_2 = -\frac{D_a(l + m_*(1 - p_n))}{D_n s}, \\ c_3 &= -\left(\frac{D_a(l + m_*(1 - p_n))}{D_n s\alpha}\right)\left(\frac{(D_n s + D_a\alpha)e^{(s/D_a)L}}{s} + \alpha L + D_n\right), \\ c_4 &= -\frac{D_a(m_* + (1 - p_c)l))}{D_c s} e^{(s/D_a)L}, \\ c_5 &= -\frac{D_a(m_* + (1 - p_c)l)}{s\beta}\left(e^{(s/D_a)L} - 1\right) - \frac{D_a^2 m_*}{D_c s^2}. \end{aligned}$$

To obtain our results, we first establish the following *a priori* estimates for nonnegative solutions of (3.11).

Lemma 3.2 *Assume that* $(A(z), N(z), C(z))$ *is a nonnegative solution of* (3.11) *with* $A, N, C \not\equiv 0$. *Then*

(1) $0 < m < m^* := r - l$;
(2) $0 < N(z) < h_1, 0 < C(z) < h_2$ *for any* $z \in [0, L]$, *where*

$$h_1 = N^0 + \frac{\alpha(r + p_n m^*)LN^0}{D_n l},\quad h_2 = C^0 + \frac{\alpha(r + p_c l)LN^0}{D_c c_n l},$$

(3) There exists a positive constant B *such that* $\|A\|_\infty \le B$ *if* $m \in (0, m^*)$.

Proof (1) Let $U = e^{-(s/D_a)z}A$. Then

$$\begin{aligned} &-D_a U''(z) - sU'(z) + (m + l)\,U = rf(N)g(C)U \ge 0,\ 0 < z < L, \\ &U'(0) = U'(L) = 0. \end{aligned}$$

By the strong maximum principle, we get $U > 0$ on $[0, L]$, and then $A > 0$ on $[0, L]$. From (3.11), we have

$$\begin{cases} -D_a A''(z) + sA'(z) - rf(N(z))g(C(z))A(z) = -(m+l)\,A(z),\ 0 < z < L, \\ D_a A'(0) - sA(0) = D_a A(L) - sA(L) = 0. \end{cases} \tag{3.14}$$

Hence the principal eigenvalue of (3.14) is $\lambda_1\left(-rf(N(\cdot))g(C(\cdot))\right) = -(m+l)$ with eigenfunction A. It follows from the monotonicity of the principal eigenvalue on the weight functions that

$$-r = \lambda_1(-r) < \lambda_1\left(-rf(N(\cdot))g(C(\cdot))\right) = -(m+l).$$

This means that $0 < m < r - l = m^*$.

(2) It follows from (3.11) that

$$\begin{aligned}
&\int_0^L \left(rf(N(z))g(C(z)) - (m+l)\right) A(z)dz = 0,\\
&\alpha(N^0 - N(L)) + \int_0^L c_n\left(p_n m - rf(N(z))g(C(z))\right) A(z)dz = 0,\\
&-\beta(C(0) - C^0) + \int_0^L \left(p_c l - rf(N(z))g(C(z))\right) A(z)dz = 0, \quad (3.15)
\end{aligned}$$

which imply that $N(L) < N^0$ and $C(0) < C^0$. Note that

$$\begin{aligned}
&-D_n N''(z) + \left(c_n r A g(C)\int_0^1 f'(sN)ds\right) N = c_n p_n m A \geq 0,\ 0 < z < L,\\
&-D_c C''(z) + \left(rAf(N)\int_0^1 g'(sC)ds\right) C = p_c l A \geq 0,\ 0 < z < L,
\end{aligned}$$

with the boundary conditions

$$\begin{aligned}
N'(0) &= 0,\ D_n N'(L) = \alpha(N^0 - N(L)) > 0,\\
-D_c C'(0) &= \beta(C^0 - C(0)) > 0,\ C'(L) = 0.
\end{aligned}$$

From the strong maximum principle, we have $N > 0$ and $C > 0$ on $[0, L]$.
It follows from (3.15) that

$$\int_0^L A(z)dz < \frac{\alpha N^0}{c_n l}.$$

For any $z \in [0, L]$, we obtain

$$\begin{aligned}
|D_n N'(z)| &= \left|D_n \int_0^z N''(x)dx\right| = \left|c_n \int_0^z \left(rf(N)g(C) - p_n m\right) A(x)dx\right|\\
&\leq \frac{\alpha(r + p_n m^*)N^0}{l},
\end{aligned}$$

and

$$
\begin{aligned}
|N(z)| &= |N(L) + N(z) - N(L)| \le |N(L)| + |N(z) - N(L)| \\
&\le N^0 + \left| \int_z^L N'(x)dx \right| \le N^0 + \frac{\alpha(r + p_n m^*)N^0}{D_n l}(L - z) \\
&< N^0 + \frac{\alpha(r + p_n m^*)LN^0}{D_n l} = h_1.
\end{aligned}
$$

On the other hand, for any $z \in [0, L]$, we get

$$
\begin{aligned}
|D_c C'(z)| &= \left| D_c \int_z^L C''(x)dx \right| = \left| \int_z^L (rf(N)g(C) - p_c l)\, A(x)dx \right| \\
&\le \frac{\alpha(r + p_c l)N^0}{c_n l},
\end{aligned}
$$

and

$$
\begin{aligned}
|C(z)| &= |C(0) + C(z) - C(0)| \le |C(0)| + |C(z) - C(0)| \\
&\le C^0 + \left| \int_0^z C'(x)dx \right| \le C^0 + \frac{\alpha(r + p_c l)N^0}{D_c c_n l}(z - 0) \\
&< C^0 + \frac{\alpha(r + p_c l)LN^0}{D_c c_n l} = h_2.
\end{aligned}
$$

(3) We now establish the boundedness of $A(z)$ for $m \in (0, m^*)$. The method used here is similar to the one used in the proof of Theorem 2.1 in Du and Hsu (2010). If it is not true, then we assume that there are a sequence $m_i \in (0, m^*)$ and corresponding positive solutions $(A_i(z), N_i(z), C_i(z))$ of (3.11) such that $\|A_i\|_\infty \to \infty$ as $i \to \infty$. Without loss of generality, we may assume that $m_i \to m_0 \in (0, m^*)$ as $i \to \infty$. From part (2), we obtain $0 < f(N_i(z))g(C_i(z)) < f(h_1)g(h_2)$ for all i and $z \in [0, L]$, and hence we also may assume $f(N_i(z))g(C_i(z)) \to \zeta(z)$ weakly in $L^2(0, L)$ for some function $\zeta(z)$ as $i \to \infty$. Let $a_i = A_i/\|A_i\|_\infty$. From the first equation of (3.11), we have

$$
\begin{cases}
-(D_a a_i'(z) - s a_i(z))' + (m_i + l)\, a_i(z) = r f(N_i(z))g(C_i(z))a_i(z),\ 0 < z < L, \\
D_a a_i'(0) - s a_i(0) = D_a a_i'(L) - s a_i(L) = 0, \\
\displaystyle\int_0^L (rf(N_i(z))g(C_i(z)) - (m_i + l))\, a_i(z)dz = 0.
\end{cases}
$$

By using L^p theory for elliptic operators and the Sobolev embedding theorem, we may assume (passing to a subsequence if necessary) that $a_i \to \xi$ in $C^1([0, L])$ as $i \to \infty$, and ξ satisfies (in the weak sense)

$$
\begin{cases}
-(D_a \xi'(z) - s\xi(z))' + (m_0 + l)\, \xi(z) = r\zeta(z)\xi(z),\ 0 < z < L, \\
D_a \xi'(0) - s\xi(0) = D_a \xi'(L) - s\xi(L) = 0, \\
\displaystyle\int_0^L (r\zeta(z) - (m_0 + l))\, \xi(z)dz = 0.
\end{cases} \tag{3.16}
$$

It follows from the strong maximum principle that $\xi > 0$ on $[0, L]$ since $\xi \geq 0$ and $\|\xi\|_\infty = 1$. Note that N_i satisfies

$$\begin{cases} \dfrac{D_n N_i''(z)}{\|A_i\|_\infty} = c_u \left(rf(N_i(z))g(C_i(z)) - p_n m_i\right) a_i(z), \ 0 < z < L, \\ N_i'(0) = 0, \ D_n N_i'(L) = \alpha(N^0 - N(L)). \end{cases} \tag{3.17}$$

Integrating (3.17) from 0 to L, we have

$$\frac{\alpha(N^0 - N(L))}{\|A_i\|_\infty} = c_n \int_0^L \left(rf(N_i(z))g(C_i(z)) - p_n m_i\right) a_i(z) dz$$

Letting $i \to \infty$ gives

$$0 = c_n \int_0^L \left(r\zeta(z) - p_n m_0\right) \xi(z) dz = c_n \int_0^L \left((1 - p_n)m_0 + l\right) \xi(z) dz > 0,$$

which is a contradiction. Hence (iii) holds.

□

We now state the existence of E_2 bifurcating from $\Gamma_0 = \{(m, 0, N^0, C^0) : m > 0\}$ at $m = m_*$ and the global bifurcation of the set of E_2 with m as parameter.

Theorem 3.3 *Assume that (3.12) holds. Then*

(i) The point $(m_*, 0, N^0, C^0)$ is a bifurcation point of the positive steady state solutions of (2.4). Moreover, near $(m_*, 0, N^0, C^0)$, there exists a positive constant $\delta > 0$ such that the bifurcating positive steady state solutions of (2.4) near $(m_*, 0, N^0, C^0)$ are on a smooth curve $\Gamma_1 = \{E_2(\tau) = (m(\tau), A(\tau, z), N(\tau, z), C(\tau, z)) : 0 < \tau < \delta\}$ with

$$\begin{cases} A(\tau, z) = \tau\bar{\varphi}(z) + o(\tau), \\ N(\tau, z) = N^0 + \tau\bar{\psi}(z) + o(\tau), \\ C(\tau, z) = C^0 + \tau\bar{\phi}(z) + o(\tau) \end{cases} \tag{3.18}$$

and $m'(0) < 0$;

(ii) m_* is the unique value for bifurcation of positive steady state solutions of (2.4) from the line of trivial solutions Γ_0;

(iii) For $\tau \in (0, \delta)$, the bifurcating solution $E_2(\tau) = (m(\tau), A(\tau, z), N(\tau, z), C(\tau, z))$ is locally asymptotically stable with respect to (2.4);

(iv) there exists a connected component Υ^+ of the set Υ of positive solutions to (3.11) such that the closure of Υ^+ includes the bifurcation point $(m_*, 0, N^0, C^0)$ and (3.11) has at least one positive solution for any $m \in (0, m_*)$.

Proof In order to obtain our results, we define function spaces

$$X_1 := \{u \in C^2[0, L] : D_a u'(0) - su(0) = D_a u'(L) - su(L) = 0\},$$
$$X_2 := \{u \in C^2[0, L] : u'(0) = 0\}, \ X_3 := \{u \in C^2[0, L] : u'(L) = 0\}, \ Y := C[0, L],$$

and a nonlinear mapping $F : \mathbb{R}^+ \times X_1 \times X_2 \times X_3 \to Y \times Y \times Y \times \mathbb{R}^2$ by

$$F(m, A(z), N(z), C(z)) = \begin{pmatrix} D_a A''(z) - sA'(z) + rf(N)g(C)A - (m+l)A \\ D_n N''(z) + p_n c_n m A - c_n r f(N) g(C) A \\ D_c C''(z) + p_c l A - r f(N) g(C) A \\ D_n N'(L) - \alpha(N^0 - N(L)) \\ D_c C'(0) - \beta(C(0) - C^0) \end{pmatrix}.$$

For any $(\varphi, \psi, \phi) \in X_1 \times X_2 \times X_3$, the Fréchet derivatives of F at (m, A, N, C) are

$$F_{(A,N,C)}(m, A(z), N(z), C(z))[\varphi, \psi, \phi] = \begin{pmatrix} D_a\varphi'' - s\varphi' + [rf(N)g(C) - (m+l)]\varphi + \dfrac{r\gamma_n A g(C)}{(\gamma_n + N)^2}\psi + \dfrac{r\gamma_c A f(N)}{(\gamma_c + C)^2}\phi \\ D_n\psi'' + c_n(p_n m - rf(N)g(C))\varphi - \dfrac{c_n r\gamma_n A g(C)}{(\gamma_n + N)^2}\psi - \dfrac{c_n r\gamma_c A f(N)}{(\gamma_c + C)^2}\phi \\ D_c\phi'' + (p_c l - rf(N)g(C))\varphi - \dfrac{r\gamma_n A g(C)}{(\gamma_n + N)^2}\psi - \dfrac{r\gamma_c A f(N)}{(\gamma_c + C)^2}\phi \\ D_n\psi'(L) + \alpha\psi(L) \\ D_c\phi'(0) - \beta\phi(0) \end{pmatrix}. \tag{3.19}$$

It is easy to see that $F(m, 0, N^0, C^0) = 0$ and

$$F_{(A,N,C)}(m_*, 0, N^0, C^0)[\varphi, \psi, \phi] = \begin{pmatrix} D_a\varphi''(z) - s\varphi'(z) \\ D_n\psi''(z) + c_n((p_n - 1)m_* - l)\varphi \\ D_c\phi''(z) - (m_* + (1 - p_c)l)\varphi \\ D_n\psi'(L) + \alpha\psi(L) \\ D_c\phi'(0) - \beta\phi(0) \end{pmatrix}. \tag{3.20}$$

Let $H := F_{(A,N,C)}(m_*, 0, N^0, C^0)$.

(i) We first show that $\dim \ker H = 1$. If $(\bar\varphi(z), \bar\psi(z), \bar\phi(z)) \in \ker H$, then

$$D_a\bar\varphi''(z) - s\bar\varphi'(z) = 0,\ 0 < z < L, \tag{3.21a}$$
$$D_n\bar\psi''(z) + c_n((p_n - 1)m_* - l)\bar\varphi(z) = 0,\ 0 < z < L, \tag{3.21b}$$
$$D_c\bar\phi''(z) - (m_* + (1 - p_c)l)\bar\varphi(z) = 0,\ 0 < z < L, \tag{3.21c}$$
$$D_n\bar\psi'(L) + \alpha\bar\psi(L) = 0, \tag{3.21d}$$
$$D_c\bar\phi'(0) - \beta\bar\phi(0) = 0. \tag{3.21e}$$

It follows from (3.21a) and $\bar\varphi \in X_1$ that $\bar\varphi(z) = e^{(s/D_a)z}$. By substituting $\bar\varphi(z)$ into (3.21b) and (3.21c) respectively and combining their boundary conditions (3.21d), (3.21e), we obtain the expression of $\bar\psi(z)$ and $\bar\phi(z)$ in (3.13). This means that

$$\dim \ker H = 1 \ \text{ and } \ \ker H = \text{span}\{(\bar\varphi(z), \bar\psi(z), \bar\phi(z))\}.$$

Next we prove that codim range $H = 1$. If $(\xi_1(z), \xi_2(z), \xi_3(z), \xi_4, \xi_5)^T \in$ range H, then there exists $(\hat{\varphi}(z), \hat{\psi}(z), \hat{\phi}(z)) \in X_1 \times X_2 \times X_3$ such that

$$\begin{aligned}
&D_a\hat{\varphi}''(z) - s\hat{\varphi}'(z) = \xi_1(z),\ 0 < z < L,\\
&D_n\hat{\psi}''(z) + c_n((p_n - 1)m_* - l)\hat{\varphi}(z) = \xi_2(z),\ 0 < z < L,\\
&D_c\hat{\phi}''(z) - (m_* + (1 - p_c)l)\hat{\varphi}(z) = \xi_3(z),\ 0 < z < L,\\
&D_n\hat{\psi}'(L) + \alpha\hat{\psi}(L) = \xi_4,\\
&D_c\hat{\phi}'(0) - \beta\hat{\phi}(0) = \xi_5.
\end{aligned} \tag{3.22}$$

Multiplying both sides of (3.21a) and the first equation of (3.22) by $\hat{\varphi}e^{-(s/D_a)z}$ and $\bar{\varphi}e^{-(s/D_a)z}$, respectively, subtracting and integrating on $[0, L]$, we have $\int_0^L \xi_1(z)\bar{\varphi}(z)e^{-(s/D_a)z}dz = 0$. Then

$$\text{range } H = \left\{(\xi_1(z), \xi_2(z), \xi_3(z), \xi_4, \xi_5) \in Y^3 \times \mathbb{R}^2 : \int_0^L \xi_1(z)\bar{\varphi}(z)e^{-(s/D_a)z}dz = 0\right\}.$$

and codim range $H = 1$.

We next prove that $F_{m,(A,N,C)}(m_*, 0, N^0, C^0)(\bar{\varphi}, \bar{\psi}, \bar{\phi}) \notin$ range H. A direct calculation gives

$$F_{m,(A,N,C)}(m_*, 0, N^0, C^0)[\bar{\varphi}(z), \bar{\psi}(z), \bar{\phi}(z)] = (-\bar{\varphi}(z), c_n p_n\bar{\varphi}(z), 0, 0, 0)^T.$$

This shows that $F_{m,(A,N,C)}(m_*, 0, N^0, C^0)(\bar{\varphi}, \bar{\psi}, \bar{\phi}) \notin$ range H since $\int_0^L \bar{\varphi}^2(z)e^{-(s/D_a)z}dz \neq 0$.

By applying the Crandall-Rabinowitz bifurcation theorem (see Crandall and Rabinowitz 1971, Theorem 1.7), we conclude that there exists a positive constant $\delta > 0$ such that all the positive steady state solutions of (2.4) lie on a smooth curve $\Gamma_1 = \{(m(\tau), A(\tau, z), N(\tau, z), C(\tau, z)) : 0 < \tau < \delta\}$ satisfying (3.18). In addition, we have

$$\begin{aligned}
m'(0) &= -\frac{\left\langle \hat{l}, F_{(A,N,C)(A,N,C)}\left(m_*, 0, N^0, C^0\right)[\varphi(z), \psi(z), \phi(z)]^2\right\rangle}{2\left\langle \hat{l}, F_{m,(A,N,C)}\left(m_*, 0, N^0, C^0\right)[\varphi(z), \psi(z), \phi(z)]\right\rangle}\\
&= -\frac{\displaystyle\int_0^L \left(\frac{r\gamma_n g(C^0)}{(\gamma_n + N^0)^2}\bar{\psi}(z) + \frac{r\gamma_c f(N^0)}{(\gamma_c + C^0)^2}\bar{\phi}(z)\right)\bar{\varphi}(z)e^{-(s/D_a)z}dz}{\displaystyle -\int_0^L \bar{\varphi}^2(z)e^{-(s/D_a)z}dz},
\end{aligned} \tag{3.23}$$

where $\hat{l}$ is a linear functional on $Y^3 \times \mathbb{R}^2$ defined as

$$\langle \hat{l}, (\xi_1(z), \xi_2(z), \xi_3(z), \xi_4, \xi_5)\rangle = \int_0^L \xi_1(z)\bar{\varphi}(z)e^{-(s/D_a)z}dz.$$

It follows from (3.13) that

$$\bar{\psi}'(z) = \frac{D_a(l + m_*(1 - p_n))}{D_n s} e^{(s/D_a)z} - \frac{D_a(l + m_*(1 - p_n))}{D_n s} \geq 0,$$
$$\bar{\phi}'(z) = \frac{D_a m_*}{D_c s} e^{(s/D_a)z} - \frac{D_a(m_* + (1 - p_c)l)}{D_c s} e^{(s/D_a)L} \leq 0$$

for $z \in [0, L]$. This implies that $\bar{\psi}(z)$ is nondecreasing and $\bar{\phi}(z)$ is nonincreasing in z. It is clear that $\bar{\psi}(L) < 0$ and $\bar{\phi}(0) < 0$. Then $\bar{\psi}(z) < 0$ and $\bar{\phi}(z) < 0$ for any $z \in [0, L]$. From (3.23) and $\bar{\varphi}(z) = e^{(s/D_a)z}$, we have $m'(0) < 0$. This completes the proof of (i).

(ii) In this installment, we will prove the uniqueness of bifurcation value m_*. Assume that $\hat{m}$ is another bifurcation value from Γ_0, then there exists a positive solutions sequence $\{(m_n, A_n, N_n, C_n)\}$ of (3.11) such that $\{(m_n, A_n, N_n, C_n)\} \to (\hat{m}, 0, N^0, C^0)$ in $C([0, L])$ as $n \to \infty$. Let $\kappa_n = A_n / \|A_n\|_\infty$. From (3.11), κ_n satisfies

$$\begin{cases} D_a \kappa_n''(z) - s\kappa_n'(z) + rf(N_n)g(C_n)\kappa_n(z) - (m_n + l)\kappa_n(z) = 0, \quad 0 < z < L, \\ D_a \kappa_n'(0) - s\kappa_n(0) = D_a \kappa_n'(L) - s\kappa_n(L) = 0. \end{cases}$$

It follows from $0 < f(N_n)g(C_n) < 1$ for all $z \in [0, L]$ that $f(N_n)g(C_n) \to f(N^0)g(C^0)$ in $C([0, L_1])$ as $n \to \infty$. Note that $\{\kappa_n\}, \{m_n\}$ are both bounded in $L^\infty[0, L]$. By using L^p theory for elliptic operators and the Sobolev embedding theorem, there exists a subsequence of $\{\kappa_n\}$, denoted by itself, and a function $\zeta \in C^2([0, L])$ such that $\kappa_n \to \zeta$ in $C^1([0, L_1])$ as $n \to \infty$, and ζ satisfies (in the weak sense)

$$\begin{cases} D_a \zeta''(z) - s\zeta'(z) + rf(N^0)g(C^0)\zeta(z) - (\hat{m} + l)\zeta(z) = 0, \quad 0 < z < L, \\ D_a \zeta'(0) - s\zeta(0) = D_a \zeta'(L) - s\zeta(L) = 0. \end{cases} \tag{3.24}$$

It follows from the strong maximum principle that $\zeta > 0$ on $[0, L]$ since $\zeta \geq 0$ and $\|\zeta\|_\infty = 1$. From (3.12) and (3.24), we have

$$\begin{cases} D_a \zeta''(z) - s\zeta'(z) + (m_* - \hat{m})\zeta(z) = 0, \qquad 0 < z < L, \\ D_a \zeta'(0) - s\zeta(0) = D_a \zeta'(L) - s\zeta(L) = 0. \end{cases} \tag{3.25}$$

Integrating from 0 to L on the both sides of the first equation of (3.25), we have

$$(m_* - \hat{m}) \int_0^L \zeta(z) dz = 0,$$

which means that $m_* = \hat{m}$.

(iii) We now consider the local stability of $E_2(\tau)$. By using the principle of exchange of stability (Corollary 1.13 and Theorem 1.16 in Crandall and Rabinowitz (1973)), there exist continuously differentiable functions

$\omega_1 : [m_*, m_* + \delta) \to \mathbb{R},\ [\varphi_1, \psi_1, \phi_1] : [m_*, m_* + \delta) \to X_1 \times X_2 \times X_3,\ \omega_2 : [0, \delta) \to \mathbb{R}$

and $[\varphi_2, \psi_2, \phi_2] : [0, \delta) \to X_1 \times X_2 \times X_3$ such that

$$\begin{aligned} &F_{(A,N,C)}\left(m, 0, N^0, C^0\right)[\varphi_1^m(z), \psi_1^m(z), \phi_1^m(z)] \\ &\quad = \omega_1(m)[\varphi_1^m(z), \psi_1^m(z), \phi_1^m(z), 0]^T, \\ &F_{(A,N,C)}\left(m(\tau), A(\tau, z), N(\tau, z), C(\tau, z)\right)[\varphi_2^\tau(z), \psi_2^\tau(z), \phi_2^\tau(z)] \\ &\quad = \omega_2(\tau)[\varphi_2^\tau(z), \psi_2^\tau(z), \phi_2^\tau(z), 0]^T \end{aligned}$$

for $z \in [0, L]$ and

$$\lim_{\tau \to 0} \frac{-\tau m'(\tau)\omega_1'(m_*)}{\omega_2(\tau)} = 1, \tag{3.26}$$

where

$$\begin{aligned} \omega_1(m_*) = \omega_2(0) = 0,\ &(\varphi_1^{m_*}(z), \psi_1^{m_*}(z), \phi_1^{m_*}(z)) = (\varphi_2^0(z), \psi_2^0(z), \phi_2^0(z)) \\ &= (\bar{\varphi}(z), \bar{\psi}(z), \bar{\phi}(z)). \end{aligned}$$

It follows from (3.19) that $\omega_1(m) = m_* - m$, and then $\omega_1'(m_*) = -1$. From (3.20) and proof of (i), $\omega_1(m_*) = 0$ is the principal eigenvalue of $F_{(A,N,C)}\left(m_*, 0, N^0, C^0\right)$. By the perturbation theory of linear operators Kato (1966), we know that $\omega_2(\tau)$ is also the principal eigenvalue of $F_{(A,N,C)}\left(m(\tau), A(\tau, z), N(\tau, z), C(\tau, z)\right)$ when τ is sufficiently small. Combining with $m'(0) < 0$ and (3.26) gives $\omega_2(\tau) < 0$ for $\tau \in [0, \delta)$. This means that $E_2(\tau)$ is locally asymptotically stable with respect to (2.4).

(iv) It is easy to see that the conditions of Theorem 3.3 and Remark 3.4 in Shi and Wang (2009) hold by using standard ways (see Shi and Wang 2009; Shi et al. 2019; Wang and Xu 2013). This means that there exists a connected component Υ^+ of Υ containing $\Gamma_1 = \{(m(\tau), A_2(\tau, z), N_2(\tau, z), C_2(\tau, z)) : 0 < \tau < \delta\}$. Moreover, the closure of Υ^+ includes the bifurcation point $(m_*, 0, N^0, C^0)$ and Υ^+ satisfies one of the following three alternatives:

1. it is not compact in $\mathbb{R} \times X_1 \times X_2 \times X_3$;
2. it contains another bifurcation point $(\hat{m}, 0, N^0, C^0)$, where $\hat{m}$ is another bifurcation value satisfying (3.21) with $\hat{m} \neq m_*$;
3. it contains a point $(m, \hat{A}(z), N^0 + \hat{N}(z), C^0 + \hat{C}(z))$, where $0 \neq (\hat{A}(z), \hat{N}(z), \hat{C}(z)) \in Z$, Z is a closed complement of $\ker L = \text{span}\{(\bar{\varphi}, \bar{\psi}, \bar{\phi})\}$ in $X_1 \times X_2 \times X_3$.

It follows from the uniqueness of bifurcation point m_* in part (ii) that case 2 cannot happen. If case 3 holds, then

$$\int_0^L \hat{A}(z)\bar{\varphi}(z)dz = 0. \tag{3.27}$$

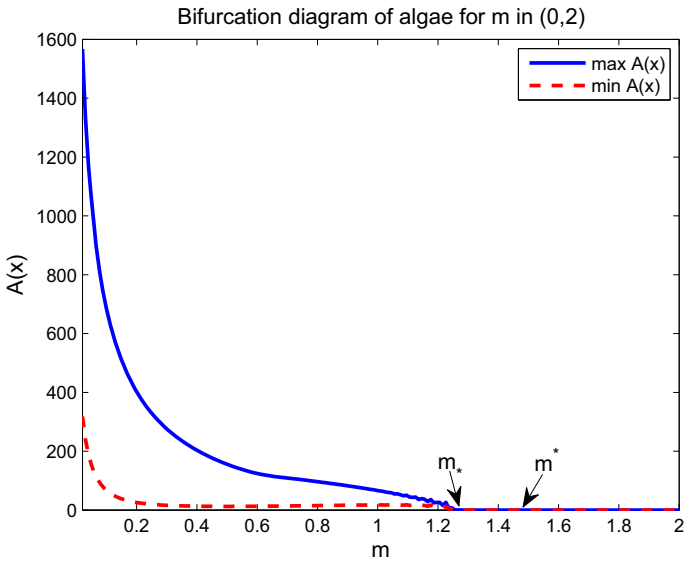

Fig. 2 Numerical bifurcation diagram of steady state algae density in (3.11) for $m \in (0, 2)$. Here $D_a = D_n = D_c = 0.1$ and other parameters except m are from Table 2, and the bifurcation values are $m^* = 1.48$ and $m_* = 1.29$

From Lemma 3.2, we have $\hat{A}(z) > 0$ on $[0, L]$, which is a contradiction to (3.27). Hence case 1 must occur for Υ^+.

From case 1, Υ^+ is unbounded in $\mathbb{R} \times X_1 \times X_2 \times X_3$. By Lemma 3.2, if $m \in (0, m^*)$, then $(A_2(z), N_2(z), C_2(z))$ is bounded. Therefore, the projection of Υ^+ onto the m-axis contains the interval $(0, m_*)$ since $m_* < m^*$. □

Theorem 3.3 shows that when $0 < m < m_*$, (2.4) always has a positive steady state solution E_2 while the nutrient-inorganic carbon-only trivial steady state E_1 is unstable from Theorem 3.1. This indicates that m_* is the threshold value for the survival and extinction of algae. It is not known whether the positive steady state solution E_2 is unique and globally asymptotically stability. It is a question worthy of further discussion in the future. In Zhang et al. (2018), the uniqueness of positive steady state was shown theoretically for the case that algae only depends on nutrient.

Next some numerical simulations are shown to illustrate our analysis of steady-states for system (2.4). Here the set of parameter values we use is derived from biologically reasonable parameters. The values of all biologically reasonable parameters are listed in Table 2.

According to Theorems 3.1 and 3.3, we can divide the parameter regime for m according to two threshold values: $m_* = rf(N^0)g(C^0) - l$ and $m^* = r - l$. E_1 always exists for all $m > 0$, and the stability of E_1 has the following three cases: (1) globally asymptotically stable when $m > m^*$, (2) locally asymptotically stable when $m_* < m < m^*$, (3) unstable when $0 < m < m_*$. The bifurcation point $m = m_*$ is a threshold value for the regime shift from extinction to survival of algae, such that

Table 2 Numerical values of parameters of model (2.4) with references

Symbol	Values	Units	Source	Symbol	Values	Units	Source
t	–	day	–	z	–	m	–
A	–	mgC/m^3	–	N	–	mgP/m^3	–
C	–	mgC/m^3	–	D_a, D_n, D_c	0.02 (0.01-10)	m^2/day	Huisman et al. (2002), Huisman et al. (2006), Jäger et al. (2010), Klausmeier and Litchman (2001), Ryabov et al. (2010)
s	0.02(-0.5-0.5)	m/day	Huisman et al. (2002), Jäger and Diehl (2014), Jäger et al. (2010), Ryabov et al. (2010), Vasconcelos et al. (2016)	r	1.5	day^{-1}	Vasconcelos et al. (2016)
m	0.1	day^{-1}	Jäger and Diehl (2014), Vasconcelos et al. (2016)	l	0.02	day^{-1}	Nie et al. (2016)
γ_n	3	mgP/m^3	Jäger and Diehl (2014), Vasconcelos et al. (2016)	γ_c	500	μmolC/m^3	Van de Waal et al. (2011)
c_n	0.008	mgP/μmolC	Jäger and Diehl (2014), Vasconcelos et al. (2016)	p_n	0.05 (0-1)	–	Assumption
p_c	0.05(0-1)	–	Assumption	α	0.05	m/day	Jäger and Diehl (2014), Vasconcelos et al. (2016)

Table 2 continued

Symbol	Values	Units	Source	Symbol	Values	Units	Source
β	0.264	m/day	Van de Waal et al. (2011)	N^0	50 (5-400)	mgP/m^3	Jäger and Diehl (2014)
C^0	6250 (500-15000)	μmolC/m^3	Van de Waal et al. (2011)	L	4	m	Assumption

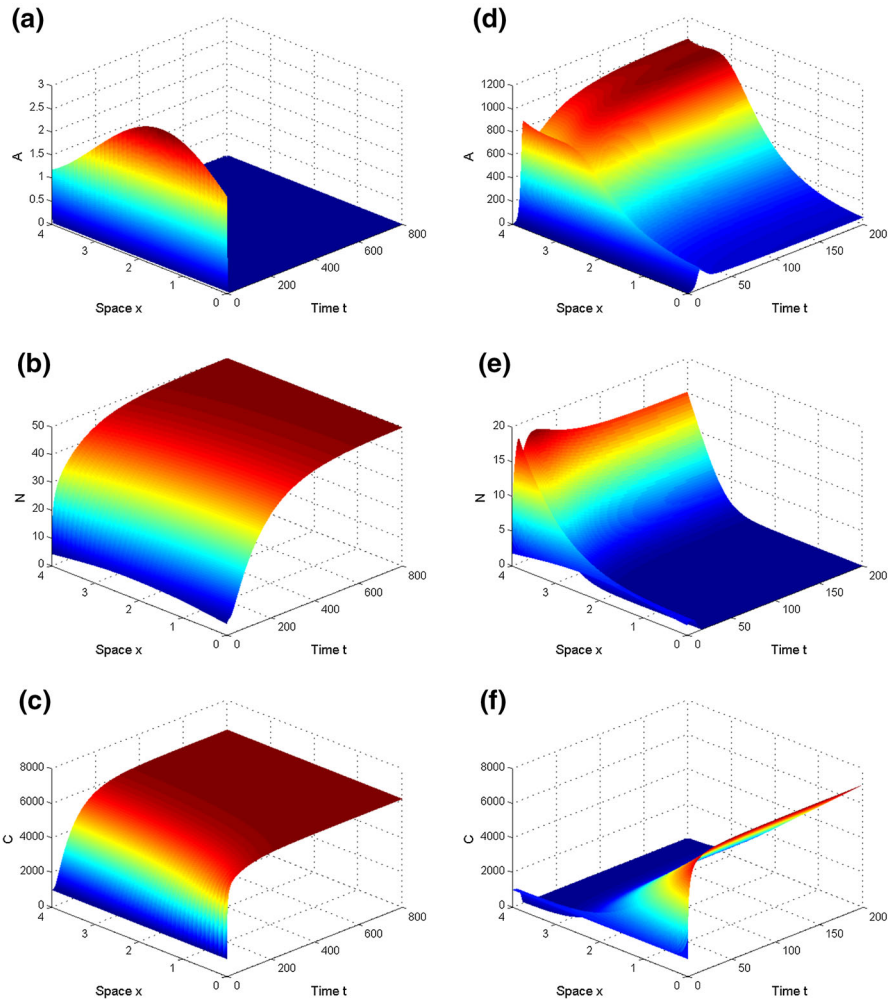

Fig. 3 Left: the solution converges to the nutrients-inorganic carbon-only trivial steady state E_1 in **a–c** with $m = 1.4$; Right: the solution converges to a positive steady state E_2 in **d–f** with $m = 0.1$. Here $D_a = D_n = D_c = 0.1$ and other parameters except m are from Table 2, and the initial conditions are $A_0(z) = 2 + \sin z$, $N_0(z) = 5 + \cos z$ and $C_0(z) = 1000$

the positive steady state solution E_2 exists when $m < m_*$ (see Fig. 2). The numerical bifurcation diagram in Fig. 2 shows that the positive steady state E_2 decreases in m.

In Fig. 3, dynamic numerical simulations of solutions of (2.4) for parameter values from Table 2 are shown. For different algal loss rates m, the solution of (2.4) converges to different steady states regardless of initial conditions. For the case of $m = 1.4 > m_*$, algae becomes extinct and the concentration of dissolved nutrients and dissolved inorganic carbon reach the concentration of dissolved nutrients at the bottom of the water column and the concentration of dissolved inorganic carbon at the surface of the water column respectively (see Theorem 3.1 and Fig. 3a–c). For the case of $m =$

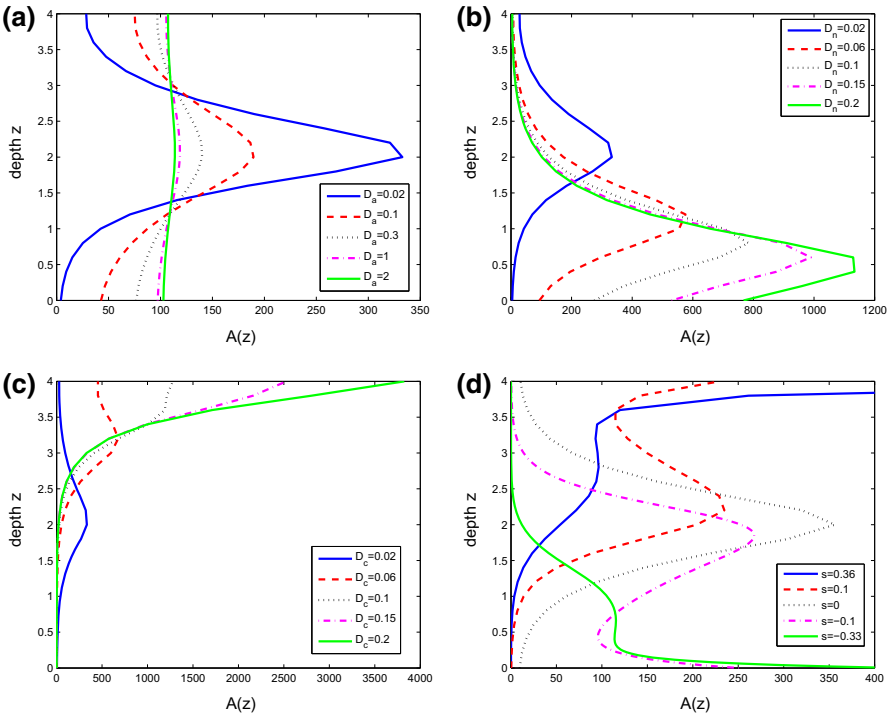

Fig. 4 Vertical distribution of the positive steady state $A(z)$ for varying D_a, D_n, D_c and s. The horizontal axis is the biomass density coordinate of algae, and the vertical axis is the depth coordinate of the water column. Here other parameters are from Table 2

$0.1 < m_*$, algae, nutrients and inorganic carbon can coexist together at a positive level (see Theorem 3.3 and Fig. 3d–f), and algae exhibit vertical aggregation phenomena (see Fig. 3d).

4 The vertical distribution of algae

The vertical distribution of algae in the aquatic ecosystem is highly heterogeneous and affects the whole aquatic ecosystem in terms of primary productivity, trophic levels and cycle of matter. Especially, algae can exhibit the most prominent vertical aggregation phenomena, where the equivalent of 90% of algal biomass sometimes gathers in a relatively thin layer (Klausmeier and Litchman 2001; Ryabov et al. 2010; Yoshiyama et al. 2009; Yoshiyama and Nakajima 2002). In the present section, we will explore the influence of environmental parameters in (2.4) on the vertical distribution of algae under the jointly limitation of nutrients and inorganic carbon when the solution of (2.4) appears to converge to a positive steady state E_2. In figures below, we compare the variation of the vertical distribution of positive steady state $A(z)$ for different parameter values.

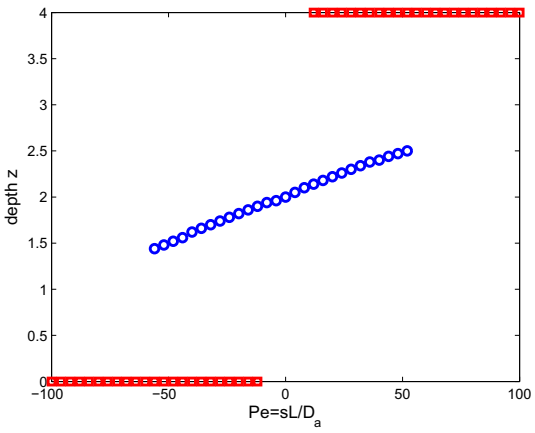

Fig. 5 Spatial location of local maxima of the positive steady state $A(z)$ for varying Peclet number (abbreviated as Pe). A red square indicates a local maximum at the boundary layer, and a blue circle indicates a local maximum at the interior. Here $s \in [-0.5, 0.5]$, $D_a = 0.02$ and other parameters are from Table 2 (colour figure online)

We first explore the effect of diffusion coefficients D_a, D_n, D_c and advection rate s on the vertical distribution of algae. It has been proved that vertical turbulent diffusivity in lake and oceans has obvious difference when the season changes Wüest and Lorke (2003). It is generally true that turbulent diffusivity is small in summer, but large in winter. From Fig. 4a, one can see that the spatial heterogeneity of algal biomass gradually changes from aggregation to even distribution when D_a increases. This confirms once again that algae are prone to aggregation in summer and not in winter because of turbulent diffusion. The increase of D_n can cause algae to gradually accumulate to the water surface, while the increase of D_c is just the opposite (see Fig. 4b and c). This is because the increase of D_a (D_c) leads to the full transfer of nutrients (organic carbon) in the water column, so that algae congregate on areas rich in inorganic carbon (nutrients). It is noted that in an aquatic ecosystem, the diffusion of algae, nutrients and inorganic carbon is a passive movement caused by turbulence in water, which only changes with turbulence. This indicates that the diffusion rates of the three are almost the same.

Suspension ($s = 0$), subsidence ($s > 0$) and floating upward ($s < 0$) of algae are not only important ways to obtain the best growth opportunities, but also greatly affect the vertical accumulation of algae. From Fig. 4d, one can observe that the vertical distribution of algae changes greatly with the decrease of s in a poorly mixed water column. For the case of $s = 0.36$ and $s = -0.33$, the algal biomass is mainly concentrated at the bottom or the surface of the water column due to the larger sinking or buoyant velocity. When $s = 0$, the maximum of the algal biomass, also described as deep chlorophyll maxima (DCMs), arises from the middle of the water column. This is because the nutrients are concentrated at the bottom, while inorganic carbon is concentrated at the surface for a lower turbulent diffusion, which leads to the optimal growth of algae in the middle of the water column. This indicates that the shift from subsidence to floating upward can cause algal blooms and bring out a large amount of algae gathering on the water surface.

Here an interesting phenomenon is the possibility of multiple local extrema of the algae vertical distribution for the smaller sinking or buoyant velocity in Fig. 4d.

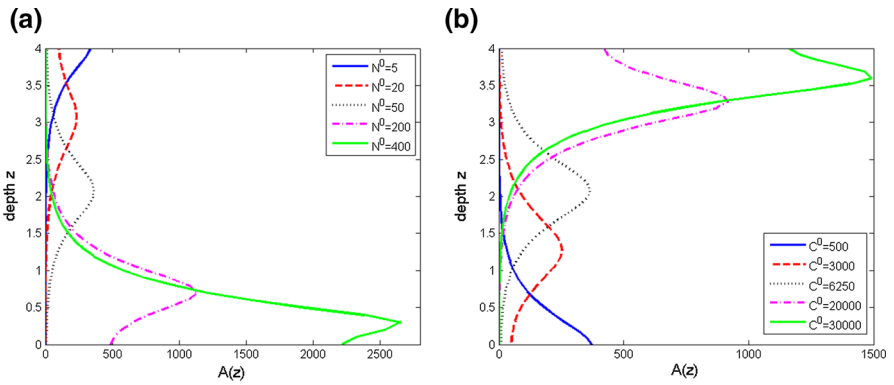

Fig. 6 Vertical distribution of the positive steady state $A(z)$ for varying N^0 (left) and C^0 (right). Here other parameters are from Table 2

For $s = 0.1$, the algal biomass is concentrated in the middle and bottom of the water column and are mainly divided into two layers: 2m-3m and 3.7m-4m. Similar phenomena also occurs for $s = -0.1$, where the algal biomass is concentrated in the middle and surface of the water column. In both cases, there are two local maximums of algae biomass density. The phenomenon of double local maxima may depend on the interplay of diffusion and advection, and the types of boundary conditions such as Robin or Dirichlet conditions on one end. Here we investigate the effect of the Peclet number on the algae vertical distribution. The Peclet number (abbreviated as Pe) is the ratio of advection rate to diffusion rate and is often used in the study of continuous transport phenomena. Figure 5 shows the locations of local maxima of the positive steady state $A(z)$ for different Peclet numbers can have five scenarios: (a) a unique local maximum at the water surface (Pe $\in (-100, -58)$); (b) two local maxima at both the water surface and the interior (Pe $\in (-58, -10)$); (c) a unique local maximum at the interior (Pe $\in (-10, 10)$); (d) two local maxima at both the bottom and the interior of water column (Pe $\in (10, 54)$); and (e) a unique local maximum at the bottom of water column (Pe $\in (54, 100)$). This phenomenon shows that there may be one or two concentration layers for the algae vertical distribution in a water column, and the variation of the algae maxima is not continuous with respect to the Peclet number.

In our model (2.4), the algal growth is limited by organic carbon and nutrients. Nutrients from the water bottom and inorganic carbon from the water surface form an asymmetric resource supply mechanism on the algal growth. An increasing concentration N^0 of dissolved nutrients at the bottom reduces the dependence of the algal growth on nutrients in the whole water column, such that the algal biomass gradually increases and the aggregation location shifts from the bottom to the surface (see Fig. 6a). When the nutrient level on the water surface is very high, algae accumulate on the water surface and algal blooms occur (see $N^0 = 400$ in Fig. 6a). Hence eutrophication of water body caused by warm conditions, industrial waste water and sewage is an important factor of algal blooms. On the other hand, increasing organic carbon causes the algal biomass vertical aggregation transfering from the surface to

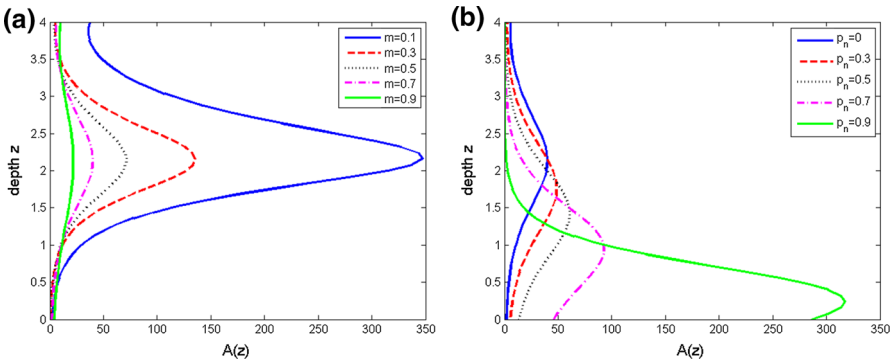

Fig. 7 Vertical distribution of the positive steady state $A(z)$ for varying m (left) and p_n (right). Here $p_n = 0$ in **a**, $m = 0.7$ in **b** and other parameters are from Table 2

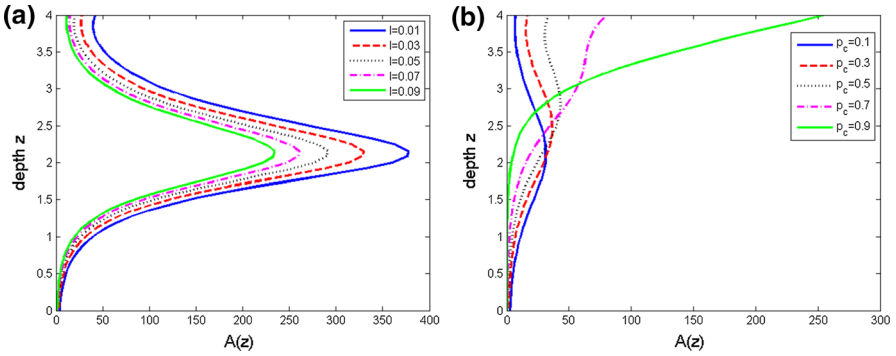

Fig. 8 Vertical distribution of the positive steady state $A(z)$ for varying l (left) and p_c (right). Here $p_c = 0$ in **a**, $l = 1.75 \times 10^{-6}$ in **b** and other parameters are from Table 2

the bottom (see Fig. 6b). This implies that the input of organic carbon can change the vertical distribution of algae, thus reduce the risk of algal blooms.

The loss rate m of algae only changes the total biomass of algae, but has no significant impact on the vertical distribution of algae (see Fig. 7a). Similarly, the respiration rate l of algae also has no essential effect on the vertical distribution of algae (see Fig. 8a). From Figs. 7b and 8b, one can observe that the nutrient recycling proportion p_n and the organic carbon recycling proportion p_c can both affect the vertical distribution of algae. It is known that algae usually carry out photosynthesis during the daytime and respiration at night. Rapid decomposition of dead algae under high daytime temperature produces enough nutrients, which leads to the increase of p_n value; on the other hand, at night, the algal respiration releases a large amount of organic carbon so that p_c increases and algae gather at the bottom. Our results in Figs. 7b and 8b are consistent with daily observation that a large amount of algae float on the surface during the daytime and sink to the bottom at night. But a full verification of this phenomenon requires a time-periodic model with night-day fluctuations, as the time scale of algae congregation dynamics is much slower than the time scale of night-day fluctuation.

Table 3 The influence of environmental parameters on $z_{\max}$, A^* and A_*

Parameters	$z_{\max}$	A^*	A_*	Parameters	$z_{\max}$	A^*	A_*
$D_a \uparrow$	—	$\uparrow$	$\uparrow$	$D_n \uparrow$	$\downarrow$	$\uparrow$	$\downarrow$
$D_c \uparrow$	$\uparrow$	$\downarrow$	$\uparrow$	$s \uparrow$	$\uparrow$	$\downarrow$	$\uparrow$
$N^0 \uparrow$	$\downarrow$	$\uparrow$	$\downarrow$	$C^0 \uparrow$	$\uparrow$	$\downarrow$	$\uparrow$
$m \uparrow$	—	$\uparrow$	$\uparrow$	$p_n \uparrow$	$\downarrow$	$\uparrow$	$\downarrow$
$l \uparrow$	—	$\uparrow$	$\uparrow$	$p_c \uparrow$	$\uparrow$	$\downarrow$	$\uparrow$

$\uparrow$: Increasing $\downarrow$: Decreasing —: No significant effect

Let $z_{\max}$ be the depth coordinate of the maximum of the algal biomass in the water column when the vertical aggregation occurs. In view of Figs. 4, 5, 6, 7, 8, $z_{\max}$ describes the change of algal aggregation layer. The increase of $z_{\max}$ indicates that algae aggregate to the deep layer, while the decrease of z_{max} indicates that algae aggregate to the surface layer. Let A^* be the algal biomass on the water surface and A_* be the algal biomass on the water bottom. Hence A^* and A_* are both important indices to measure algal blooms and the change of water quality. As a summary of the above discussion (see Figs. 4, 5, 6, 7, 8), the influence of environmental parameters on $z_{\max}$, A^* and A_* are listed in Table 3.

5 Discussion

We propose a reaction-diffusion-advection model (2.4) to describe the dynamic interactions among algae, nutrients and inorganic carbon in a water column. The algal growth depends on limited nutrients from the water bottom and limited inorganic carbon from the water surface, which is an asymmetric supply of resources. The threshold condition for the regime shift from extinction to existence of algae is rigorously derived.

Our studies suggest that algae can exhibit vertical spatial heterogeneity and vertical aggregation in the water column under the joint effect of nutrient and inorganic carbon supply (see Figs. 4, 5, 6, 7, 8 and Table 3). This is a new discovery and rarely noticed in the existing studies. It shows that the asymmetric resource supply, such as nutrients and inorganic carbon in the present paper, and nutrients and light in previous studies (Du and Hsu 2008a, b; Klausmeier and Litchman 2001; Yoshiyama et al. 2009), is an important factor for the vertical distribution of algae. Another interesting phenomenon observed from numerical simulation of our model is that there are possibly one or two local maxima of the vertical distribution of algae, while there is usually a unique maximum concentration point for the algae vertical distribution in algae-nutrient model (Hsu et al. 2013; Nie et al. 2015; Shi et al. 2019; Wang et al. 2015; Zhang et al. 2018) or algae-inorganic carbon model (Hsu et al. 2017; Nie et al. 2016). This indicates that the possibility of multiple algal accumulation zones in a water column under the mechanism of asymmetric supply of nutrients and inorganic carbon. These findings are useful for assessing algal blooms and protecting aquatic ecosystems.

In the theoretical analysis, we establish theoretical results showing that algae become extinct when the loss rate m exceeds the threshold value m_*, while algae

invade and persist when m is below the threshold value m_*. But there are still some remaining questions in model (2.4). From Theorems 3.1 and 3.3, together with the bifurcation diagram (Fig. 2), we conjecture that E_1 is globally asymptotically stable if $m > m_*$, and E_2 is globally asymptotically stable if $m < m_*$. Figs. 4, 5, 6, 7, 8 show that the profile of the positive steady state $A(z)$ has a complex pattern for varying environmental parameters. Especially, the number of locations of local maxima of algae distribution at the boundary and interior are related to Peclet number and Damköhler number. The Damköhler number is used to describe the relative time scale of chemical reactions in the same system compared with other phenomena. It is usually defined as the ratio of chemical time scale to mixed time scale. Rigorously proving these results is an interesting and important question. It may need some new methods and special techniques.

In Hsu et al. (2017), Nie et al. (2016), the authors considered the interaction between algae and inorganic carbon in a poorly mixed habitat. They divided inorganic carbon into two parts: CO_2 and CARB (bicarbonate and carbonate ions). CO_2 and CARB are two substitutable resources. The two parts can be converted to each other in the water column. Their models should be more reasonable in describing the interaction between algae and inorganic carbon. In model (2.4), we simplify the above relationship and unify CO_2 and CARB into inorganic carbon for the purpose of this study. The main purpose of the present paper is to investigate the vertical distribution and aggregation of algae under the mechanism of asymmetric supply of nutrients and inorganic carbon. Hence we did not consider the more complex mechanism in inorganic carbon. It is important and of interest to add this complex mechanism in inorganic carbon into model (2.4), and maybe some new dynamic behaviors will be generated.

Light is one of the essential resources for algal growth (Du and Hsu 2010; Du et al. 2015; Hsu and Lou 2010; Peng and Zhao 2016). Concentrating on the research motivation of the current model, we neglect the role of light (assuming sufficient light) in model (2.4). An important and interesting problem is to study the growth model and vertical distribution of algae under the combined action of light, nutrients and inorganic carbon. Based on the present discussion and model (2.4), it will be of interest to explore more biological questions. For example, two or more algae compete for nutrients and inorganic carbon; the effect of toxic plankton species, zooplankton and fishes, stoichiometric algal growth model with nutrients and inorganic carbon.

Acknowledgements The authors would like to thank two anonymous reviewers for careful reading of the manuscript and for important suggestions and comments, which led to the improvement of our manuscript. This work was done when the first and third authors visited Department of Mathematics, William & Mary during the academic year 2019-2020, and they would like to thank Department of Mathematics, William & Mary for their support and warm hospitality.

References

Chen M, Fan M, Liu R, Wang XY, Yuan X, Zhu HP (2015) The dynamics of temperature and light on the growth of phytoplankton. J Theor Biol 385(21):8–19

Crandall MG, Rabinowitz PH (1971) Bifurcation from simple eigenvalues. J Funct Anal 8(2):321–340

Crandall MG, Rabinowitz PH (1973) Bifurcation, perturbation of simple eigenvalues and linearized stability. Arch Rational Mech Anal 52(2):161–180

Du YH, Hsu SB (2008) Concentration phenomena in a nonlocal quasi-linear problem modelling phytoplankton. I. Exist SIAM J Math Anal 40(4):1419–1440
Du YH, Hsu SB (2008) Concentration phenomena in a nonlocal quasi-linear problem modelling phytoplankton. II. Limiting Profile SIAM J Math Anal 40(4):1441–1470
Du YH, Hsu SB (2010) On a nonlocal reaction-diffusion problem arising from the modeling of phytoplankton growth. SIAM J Math Anal 42(3):1305–1333
Du YH, Hsu SB, Lou Y (2015) Multiple steady-states in phytoplankton population induced by photoinhibition. J Differ Equ 258(7):2408–2434
Grover JP (1997) Resource competition. Chapman and Hall, London
Grover JP (2017) Sink or swim? vertical movement and nutrient storage in phytoplankton. J Theor Biol 432(7):38–48
Heggerud CM, Wang H, Lewis MA (2020) Transient Dynamics of a stoichiometric cyanobacteria model via multiple-scale analysis. SIAM J Appl Math 80(3):1223–1246
Henry D (1981) Geometric theory of semilinear parabolic equations. Lecture Notes in Mathematics, vol 840. Springer-Verlag, Berlin-New York
Hsu SB, Lam KY, Wang FB (2017) Single species growth consuming inorganic carbon with internal storage in a poorly mixed habitat. J Math Biol 75(6–7):1775–1825
Hsu SB, Lou Y (2010) Single phytoplankton species growth with light and advection in a water column. SIAM J Appl Math 70(8):2942–2974
Hsu SB, Wang FB, Zhao XQ (2013) Global dynamics of zooplankton and harmful algae in flowing habitats. J Differ Equ 255(3):265–297
Hsu SB, Wang FB, Zhao XQ (2016) Competition for two essential resources with internal storage and periodic input. Differ Integral Equ 29(7/8):601–630
Huisman J, Arrayás M, Ebert U, Sommeijer B (2002) How do sinking phytoplankton species manage to persist? Am Nat 159(3):245–254
Huisman J, Arrayás M, Ebert U, Sommeijer B (2006) Reduced mixing generates oscillations and chaos in the oceanic deep chlorophyll maximum. Nature 439(7074):322
Jäger CG, Diehl S (2014) Resource competition across habitat boundaries: asymmetric interactions between benthic and pelagic producers. Ecol Monogr 84(2):287–302
Jäger CG, Diehl S, Emans M (2010) Physical determinants of phytoplankton production, algal stoichiometry, and vertical nutrient fluxes. Am Nat 175(4):91–104
Jiang DH, Lam KY, Lou Y, Wang ZC (2019) Monotonicity and global dynamics of a nonlocal two-species phytoplankton model. SIAM J Appl Math 79(2):716–742
Kato T (1966) Perturbation theory for linear operators. Springer-Verlag, Berlin-New York
Klausmeier CA, Litchman E (2001) Algal games: the vertical distribution of phytoplankton in poorly mixed water columns. Limnol Oceanogr 46(8):1998–2007
Klausmeier CA, Litchman E, Levin SA (2004) Phytoplankton growth and stoichiometry under multiple nutrient limitation. Limnol Oceanogr 49(4):1463–1470
Mei LF, Zhang XY (2012) Existence and nonexistence of positive steady states in multi-species phytoplankton dynamics. J Differ Equ 253(7):2025–2063
Mischaikow K, Smith H, Thieme HR (1995) Asymptotically autonomous semiflows: chain recurrence and Lyapunov functions. Trans Am Math Soc 347(5):1669–1685
Nie H, Hsu SB, Grover JP (2016) Algal competition in a water column with excessive dioxide in the atmosphere. J Math Biol 72(7):1845–1892
Nie H, Hsu SB, Wu JH (2015) Coexistence solutions of a competition model with two species in a water column. Discrete Contin Dyn Syst Ser B 20(8):2691–2714
Peng R, Zhao XQ (2016) A nonlocal and periodic reaction-diffusion-advection model of a single phytoplankton species. J Math Biol 72(3):755–791
Ryabov AB, Rudolf L, Blasius B (2010) Vertical distribution and composition of phytoplankton under the influence of an upper mixed layer. J Theor Biol 263(1):120–133
Shi JP, Wang XF (2009) On global bifurcation for quasilinear elliptic systems on bounded domains. J Differ Equ 246(7):2788–2812
Shi JP, Zhang JM, Zhang XY (2019) Stability and asymptotic profile of steady state solutions to a reaction-diffusion pelagic-benthic algae growth model. Commun Pure Appl Anal 18(5):2325–2347
Thieme HR (1992) Convergence results and a poincaré-bendixson trichotomy for asymptotically autonomous differential equations. J Math Biol 30(7):755–763

Van de Waal D, Verspagen JMH, Finke JF, Vournazou V, Immers AK, Kardinaal WEA, Tonk L, Becker S, Van Donk E, Visser PM, Huisman J (2011) Reversal in competitive dominance of a toxic versus non-toxic cyanobacterium in response to rising CO_2. ISME J 5(9):1438–1450

Vasconcelos FR, Diehl S, Rodríguez P, Hedström P, Karlsson J, Byström P (2016) Asymmetrical competition between aquatic primary producers in a warmer and browner world. Ecology 97(10):2580–2592

Wang FB, Hsu SB, Zhao XQ (2015) A reaction-diffusion-advection model of harmful algae growth with toxin degradation. J Differ Equ 259(7):3178–3201

Wang H, Smith HL, Kuang Y, Elser JJ (2007) Dynamics of stoichiometric bacteria-algae interactions in the epilimnion. SIAM J Appl Math 68(2):503–522

Wang XF, Xu Q (2013) Spiky and transition layer steady states of chemotaxis systems via global bifurcation and Helly's compactness theorem. J Math Biol 66(6):1241–1266

Wüest A, Lorke A (2003) Small-scale hydrodynamics in lakes. Ann Rev Fluid Mech 35(1):373–412

Yoshiyama K, Mellard JP, Litchman E, Klausmeier CA (2009) Phytoplankton competition for nutrients and light in a stratified water column. Am Nat 174(2):190–203

Yoshiyama K, Nakajima H (2002) Catastrophic transition in vertical distributions of phytoplankton: alternative equilibria in a water column. J Theor Biol 216(4):397–408

Zagaris A, Doelman A (2011) Emergence of steady and oscillatory localized structures in a phytoplankton-nutrient model. Nonlinearity 24(12):3437–3486

Zhang JM, Kong JD, Shi JP, Wang H (2021) Phytoplankton competition for nutrients and light in a stratified lake: a mathematical model connecting epilimnion and hypolimnion. J Nonlinear Sci 31:35

Zhang JM, Shi JP, Chang XY (2018) A mathematical model of algae growth in a pelagic-benthic coupled shallow aquatic ecosystem. J Math Biol 76(5):1159–1193